Pentafluorophenylphosphine Complexes of Rhodium(I): Extended X-Ray Absorption Fine Structure Studies of $[\{Rh[PPh_x(C_6F_5)_{3-x}]_2(\mu\text{-}Cl)\}_n]$ (x = 0–2) and $[\{Rh[(C_6F_5)_2PCH_2CH_2P(C_6F_5)_2](\mu\text{-}Cl)\}_2]$. Crystal Structures of $[RhCl(PPh_3)\{(C_6F_5)_2PCH_2CH_2P(C_6F_5)_2\}]\cdot C_4H_8O$ and $(C_6F_5)_2PCH_2CH_2P(C_6F_5)_2$†

Malcolm J. Atherton,[a] Karl S. Coleman,[b] John Fawcett,[b] John H. Holloway,[b] Eric G. Hope,[b] Atilla Karaçar,[b] Lee A. Peck[b] and Graham C. Saunders*[,b]

[a] *BNFL Fluorochemicals Ltd., Springfields, Salwick, Preston PR4 0XJ, UK*

[b] *Department of Chemistry, The University, Leicester LE1 7RH, UK*

The NMR spectroscopic properties of the rhodium pentafluorophenylphosphine complexes $[\{Rh[PPh_x(C_6F_5)_{3-x}]_2(\mu\text{-}Cl)\}_n]$ (x = 0 **1**, 1 **2** or 2 **3**) and *trans*-$[Rh\{PPh_x(C_6F_5)_{3-x}\}_2Cl(CO)]$ (x = 0 **5**, 1 **6** or 2 **7**) have been investigated. The new complexes $[\{Rh[(C_6F_5)_2PCH_2CH_2P(C_6F_5)_2](\mu\text{-}Cl)\}_2]$ **4** and *cis*-$[Rh\{(C_6F_5)_2PCH_2CH_2P(C_6F_5)_2\}Cl(CO)]$ **8** have been prepared. A rhodium K-edge extended X-ray absorption fine structure (EXAFS) study of complexes **1**–**4** has been performed, and confirms that complexes **2**, **3** and **4** are dimers with each Rh ··· Rh' distance bridged by two chlorides [d(Rh–P) 2.16–2.21, d(Rh–Cl) 2.38–2.39, d(Rh ··· Rh') 3.50–3.58 Å], whereas complex **1** is a polymer with each Rh ··· Rh' distance bridged by one chloride [d(Rh–P) 2.18, d(Rh–Cl) 2.36, d(Rh ··· Rh') 4.30 Å]. The reaction between $[\{Rh[(C_6F_5)_2PCH_2CH_2P(C_6F_5)_2](\mu\text{-}Cl)\}_2]$ and PPh_3 yields the four-co-ordinate mononuclear rhodium(I) complex $[RhCl(PPh_3)\{(C_6F_5)_2PCH_2CH_2P(C_6F_5)_2\}]$ **9**. The crystal structures of **9** and of $(C_6F_5)_2PCH_2CH_2P(C_6F_5)_2$ have been determined by X-ray crystallography. Complex **9** crystallizes in the monoclinic space group $P2_1/c$ with a = 12.707(2), b = 17.066(2), c = 22.003(3) Å, β = 101.41(1)°, Z = 4. Refinement gave final R_1 and wR_2 values of 0.0429 and 0.0715 for 5193 observed reflections. The geometry about the rhodium atom is distorted-square planar and there is a short distance between an *ortho*-hydrogen atom of the triphenylphosphine ligand and the rhodium atom (2.699 Å) indicative of an agostic interaction. The phosphine $(C_6F_5)_2PCH_2CH_2P(C_6F_5)_2$ crystallizes in the triclinic space group $P\bar{1}$ with a = 5.833(1), b = 10.011(2), c = 11.514(4) Å, α = 75.25(2), β = 88.69(2), γ = 84.28(2)°, Z = 1. Refinement gave final R_1 and wR_2 values of 0.0482 and 0.0987 respectively for 1339 observed reflections.

The presence of fluorine in strategic positions in phosphorus(III) ligands can have a profound impact on the nature of the complexes they form. Transition-metal complexes of the phenylphosphines $P(C_6F_5)_3$, $PPh(C_6F_5)_2$ and $PPh_2(C_6F_5)$ [1–5] and the phenyl phosphite, phenyl phosphonite and phenyl phosphinite ligands $P(OC_6H_3F_2\text{-}2,6)_3$,[6,7] $PPh(OC_6H_3F_2\text{-}2,6)_2$[5] and $PPh_2(OC_6H_3F_2\text{-}2,6)$[5] possess significantly different chemical and structural properties from those of their perprotio analogues. As part of our study into the effect of *ortho*-fluorines in phenylphosphine ligands we have investigated pentafluorophenylphosphine complexes of rhodium. The complexes $[\{Rh[PPh_x(C_6F_5)_{3-x}]_2(\mu\text{-}Cl)\}_n]$ (x = 0 **1**, 1 **2** or 2 **3**) and *trans*-$[Rh\{PPh_x(C_6F_5)_{3-x}\}_2Cl(CO)]$ (x = 0 **5**, 1 **6** or 2 **7**) have been known for some time.[1,2,8] Their ^{19}F NMR spectra were reported, but the ^1H and ^{31}P NMR spectra have not been described. Furthermore, the complexes were not structurally characterized. The dimeric nature of complexes **1**–**3** was inferred from the IR spectra and molecular weight determinations, but the difference in properties between the dark green, insoluble complex **1** and the red, highly soluble complexes **2** and **3** casts doubt over the correctness of their formulations. The geometries of complexes **5**, **6** and **7** were assigned as *trans*-square-planar on the basis that ν(C≡O) for solutions of the complexes were *ca.* 5 cm^{-1} lower in benzene than in chloroform. We have reinvestigated these complexes in order to determine their structures.

Here we report the ^1H and ^{31}P NMR spectra of the complexes and the related complexes $[\{Rh[(C_6F_5)_2PCH_2CH_2P(C_6F_5)_2](\mu\text{-}Cl)\}_2]$ **4**, $[Rh\{(C_6F_5)_2PCH_2CH_2P(C_6F_5)_2\}Cl(CO)]$ **8** and $[RhCl(PPh_3)\{(C_6F_5)_2PCH_2CH_2P(C_6F_5)_2\}]$ **9**, and structural studies of **1**–**4**, **9** and the phosphine $(C_6F_5)_2PCH_2CH_2P(C_6F_5)_2$ (dfppe).

Results and Discussion

Compounds **1**–**3** were prepared by treatment of $[Rh\{(\eta^2\text{-}C_2H_4)_2(\mu\text{-}Cl)\}_2]$ with $P(C_6F_5)_3$, $PPh(C_6F_5)_2$ and $PPh_2(C_6F_5)$ respectively (see Scheme 1). Compound **1** is a dark green solid, insoluble in all common solvents. In contrast, compounds **2** and **3** are highly soluble red solids, which were characterized by comparison of their spectra with those reported.[2] The ^1H, ^{19}F and $^{31}P\text{-}\{^1H\}$ NMR spectroscopic data and mass spectral data are presented in Table 1. Compound **1** was found to give no mass spectral signal assignable to $Rh\{P(C_6F_5)_3\}$ species, and was too insoluble for a NMR spectroscopic study. What was believed to be the ^{19}F NMR spectrum of **1** has been reported,[2] but our study suggests this may be that of a soluble impurity or decomposition product of **1** in the NMR solvent. The mass

† *Supplementary data available:* see Instructions for Authors, *J. Chem. Soc., Dalton Trans.*, 1995, Issue 1, pp. xxv–xxx.

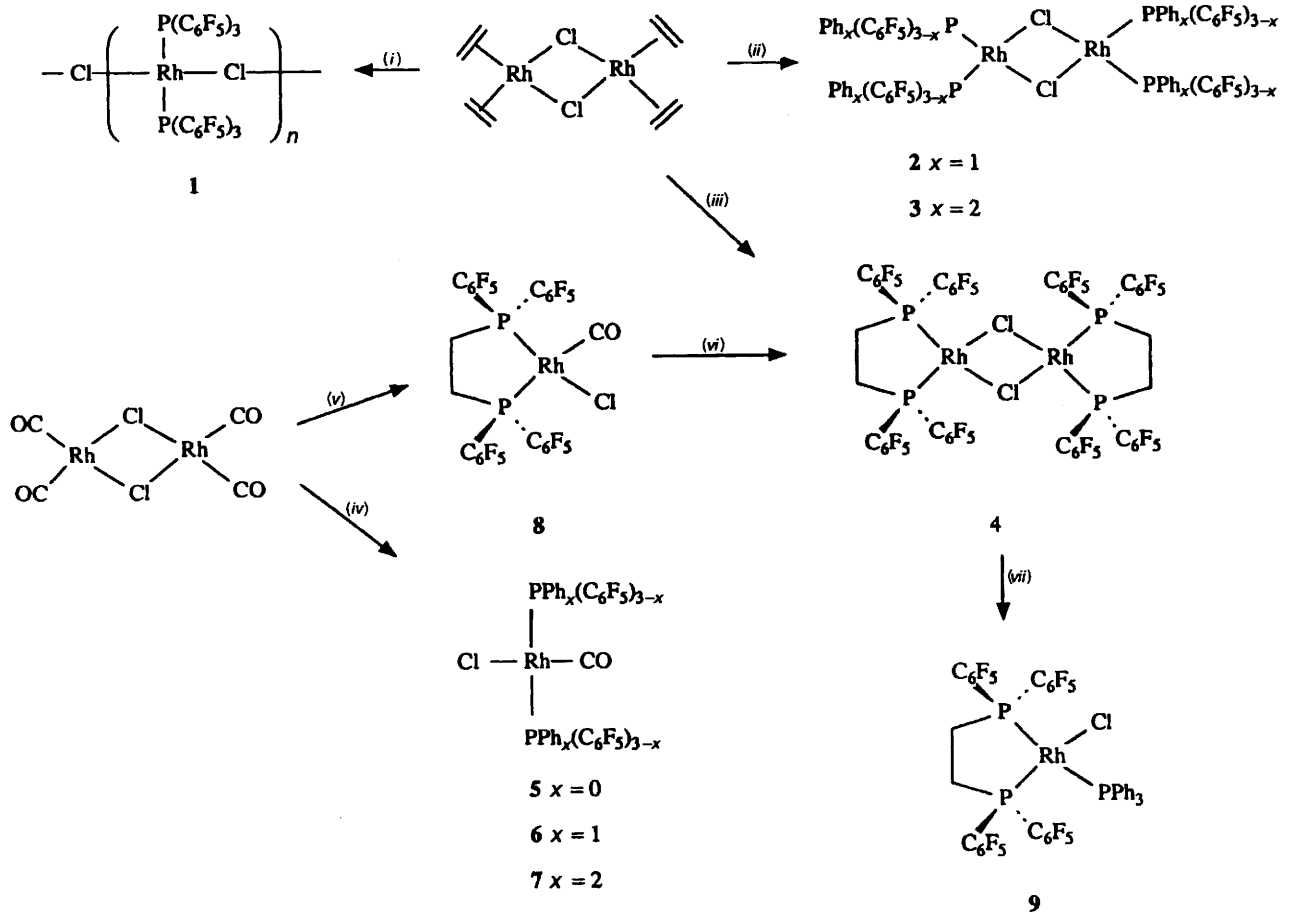

Scheme 1 (*i*) $P(C_6F_5)_3$, MeOH, heat. (*ii*) $PPh_x(C_6F_5)_{3-x}$ (x = 1 or 2), MeOH, heat. (*iii*) $(C_6F_5)_2PCH_2CH_2P(C_6F_5)_2$, CH_2Cl_2. (*iv*) $PPh_x(C_6F_5)_{3-x}$ (x = 0, 1 or 2), CH_2Cl_2. (*v*) $(C_6F_5)_2PCH_2CH_2P(C_6F_5)_2$, CH_2Cl_2. (*vi*) heat. (*vii*) PPh_3, CH_2Cl_2

spectral data of complexes **2** and **3** strongly suggest that these are dimers, $[\{Rh[PPh_x(C_6F_5)_{3-x}]_2(\mu\text{-}Cl)\}_2]$. The similarity of complexes **2** and **3** is reflected in their $^{31}P\text{-}\{^1H\}$ NMR spectra. Both exhibit doublets with coupling constants, $^1J(RhP)$, of *ca.* 200 Hz shifted to higher frequency by *ca.* 70 ppm from the resonances of the free ligands. The analogous triphenylphosphine complex, $[\{Rh(PPh_3)_2(\mu\text{-}Cl)\}_2]$, exhibits a doublet with a coupling, $^1J(RhP)$, of 193.2 Hz at *ca.* 60 ppm higher frequency than that of PPh_3.[9] The different appearance and solubility of complex **1** suggest that it does not have the same formulation.

The new complex $[\{Rh[(C_6F_5)_2PCH_2CH_2P(C_6F_5)_2](\mu\text{-}Cl)\}_2]$ **4** was prepared by treatment of $[\{Rh(\eta^2\text{-}C_2H_4)_2(\mu\text{-}Cl)\}_2]$ with $(C_6F_5)_2PCH_2CH_2P(C_6F_5)_2$ (dfppe). Complex **4** is an air-stable orange solid, readily soluble in polar organic solvents, and was characterized by elemental analysis, IR spectroscopy, mass spectrometry and ^1H, ^{19}F and $^{31}P\text{-}\{^1H\}$ NMR spectroscopies (Table 1). In appearance and solubility complex **4** resembles complexes **2** and **3**, and the mass spectral data suggest that it is also a dinuclear species.

The complete insolubility of **1** and the very high solubilities of **2**–**4** have precluded all attempts to obtain crystals suitable for X-ray structural determinations. However, extended X-ray absorption fine structure (EXAFS), in combination with spectroscopic studies, has been widely used for structural identification in metal–phosphine–halide complexes when single crystals have been unavailable.[10] For **2**–**4**, our spectroscopic investigations suggested chloride-bridged dimeric structures and initially we obtained the rhodium K-edge EXAFS data for the structurally characterized, dimeric complex $[\{Rh(PPh_3)_2(\mu\text{-}Cl)\}_2]$[11] as a model system to test the reliability of our data collection and treatment (Fig. 1). The results are in very satisfactory agreement with the single-crystal X-ray data (Table 2). The Fourier transform of the EXAFS is dominated by back-scattering from bonded phosphorus and chlorine atoms which give the Rh–P distance as 2.20 Å as compared to 2.206 Å (mean) from the X-ray single crystal study and the Rh–Cl distance as 2.37 Å as compared to 2.409 Å (mean). Additional features beyond 3.0 Å include the non-bonded Rh · · · C(phenyl) distances (see footnote to Table 2) which are in reasonable agreement with the non-bonded Rh · · · C(phenyl) distances calculated from the X-ray single crystal data, and most importantly a *single* Rh · · · Rh′ distance at 3.65 Å which compares with 3.662 Å from the single-crystal work, confirming the dimeric structure of this complex.

Transmission Rh K-edge EXAFS were then collected for complexes **1**–**4** out to k = 15 Å^{-1} (k = photoelectron wave vector) beyond the edge but, due to poor signal/noise at high k, the data were usually truncated at 13.5 Å^{-1}. Several data sets on each compound were averaged, and the data multiplied by k^3 to compensate for the fall off in intensity at higher k. No smoothing or Fourier filtering was applied, and the fits discussed below were all compared with the average raw (background-subtracted) EXAFS data. As with the model compound, the Fourier transforms were dominated by two near coincident shells at *ca.* 2.2 Å and, in all cases, were initially modelled to two shells of two phosphorus and two chlorine atoms at *ca.* 2.2 and 2.4 Å respectively. Throughout, d(Rh–P) was shorter than d(Rh–Cl) and reversing these shells gave a 10% increase in the R factor and unreasonable values for the Debye–Waller factors for both shells. Although the EXAFS analysis is fairly insensitive to co-ordination numbers, typically an accuracy of ± 10% is often quoted, it has been shown recently that accurate information on co-ordination numbers can be obtained from a careful analysis of the data.[12] The co-

Table 1 Mass spectral and NMR spectral data for compounds **2–9**

Compound	m/z[a]	NMR[b]
2	2045 (M^+)	^{1}H: 7.17 (12 H, m, C_6H_5), 6.93 (8 H, m, C_6H_5) ^{19}F: −125.79 (16 F, m, F_o), −150.13 (8 F, m, F_p), −161.49 (16 F, m, F_m) ^{31}P-{^{1}H}: 20.82 [dm, ^1J(RhP) 201.0]
3	1685 (M^+)	^{1}H: 7.63 (16 H, m, H_m or H_o), 7.23 [8 H, tm, $^3J(H_mH_p)$ 7.2, H_p], 7.07 (16 H, vtm, J 7.5, H_m or H_o) ^{19}F: −124.31 [8 F, dm, $^3J(F_oF_m)$ 21.1, F_o], −152.16 [4 F, tm, $^3J(F_mF_p)$ 22.0, F_p], −162.19 (8 F, vtm, J 19.2, F_m) ^{31}P-{^{1}H}: 42.29 [dm, ^1J(RhP) 200.0]
4[c]	1792 (M^+)	^{1}H: 2.62 [8 H, dm, ^2J(PH) 22.1, CH_2] ^{19}F: −129.43 [16 F, dm, $^3J(F_oF_m)$ 19.95, F_o], −148.49 [8 F, t, $^3J(F_mF_p)$ 20.2, F_p], −159.88 (16 F, vt, J 19.5, F_m) ^{31}P: 41.85 [dtm, ^1J(RhP) 208.5, ^2J(PH) 22.1]
5[d]	1230 (M^+) 1202 [$(M - CO)^+$]	^{19}F: −126.42 (12 F, m, F_o), −144.95 [6 F, tm, $^3J(F_mF_p)$ 20.7, F_p], −158.61 (12 F, m, F_m) ^{31}P: −25.84 [dm, ^1J(RhP) 155.3]
6[e]	1050 (M^+) 1022 [$(M - CO)^+$]	^{1}H: 7.77 (4 H, m, C_6H_5), 7.47 (6 H, m, C_6H_5) ^{19}F: −125.18 [8 F, dm, $^3J(F_oF_m)$ 21.0, F_o], −147.34 [4 F, tt, $^3J(F_mF_p)$ 20.7, $^4J(F_oF_p)$ 5.3, F_p], −159.63 (8 F, vtm, J 20.7, F_m) ^{31}P-{^{1}H}: 3.40 [dm, ^1J(RhP) 136.4]
7[f]	870 (M^+) 842 [$(M - CO)^+$]	^{1}H: 7.83 (8 H, vq, J 6.3, C_6H_5), 7.46 (12 H, m, C_6H_5) ^{19}F: −124.77 [4 F, dm, $^3J(F_oF_m)$ 20.8, F_o], −149.30 [2 F, tm, $^3J(F_mF_p)$ 20.8, F_p], −160.9 (4 F, m, F_m) ^{31}P-{^{1}H}: 24.02 [dm, ^1J(RhP) 133.0]
8[g]		^{1}H: 2.90 [4 H, dm, ^2J(PH) 24.0, CH_2] ^{19}F: −126.34 [4 F, dm, $^3J(F_oF_m)$ 18.1, F_o], −130.32 [4 F, dm, $^3J(F_oF_m)$ 13.7, F_o], −144.90 (2 F, m, F_p), −145.66 (2 F, m, F_p), −157.56 (4 F, m, F_m), −158.06 (4 F, m, F_m) ^{31}P-{^{1}H}: 34.94 [ddm, ^1J(RhP) 189.1, ^2J(PP) *ca.* 30], 33.66 [ddm, ^1J(RhP) 219.6, ^2J(PP) *ca.* 30]
9[h]	1158 [$(M + H)^+$] 1123 [$(M - Cl + H)^+$]	^{1}H: 7.48 (6 H, vt, J 8.3, PPh_3), 7.33 (3 H, m, PPh_3), 7.25 (6 H, m, PPh_3), 2.74 [2 H, dm, ^2J(PH) 29.5, CH_2], 2.43 [2 H, dm, ^2J(PH) 31.1, CH_2] ^{19}F: −127.57 [4 F, d, $^3J(F_oF_m)$ 21.3, F_o], −128.00 [4 F, d, $^3J(F_oF_m)$ 22.5, F_o], −148.16 [2 F, t, $^3J(F_pF_m)$ 20.95, F_p], −148.49 [2 F, t, $^3J(F_pF_m)$ 20.9, F_p], −159.99 (8 F, m, F_m) ^{31}P-{^{1}H}: ABCX pattern 33.0

[a] Fast-atom bombardment with *m*-nitrobenzyl alcohol matrix. [b] Recorded in $CDCl_3$. Data given as: chemical shift (δ) [relative intensity, multiplicity (J in Hz), assignment], d = doublet, t = triplet, vt = virtual triplet, vq = virtual quartet, m = multiplet. [c] Analysis found: C, 34.9; H, 0.35; Cl, 3.7; P, 6.3. $C_{52}H_8Cl_2F_{40}P_4Rh$ requires C, 34.8; H, 0.45; Cl, 3.95; P, 6.9%. [d] ν(C≡O) 2008 cm^{-1}. [e] ν(C≡O) 2002 cm^{-1}. [f] ν(C≡O) 1982 cm^{-1}. [g] ν(C≡O) 2009 cm^{-1}. [h] Analysis found: C, 45.6; H, 1.6; Cl, 2.6; P, 7.3. $C_{44}H_{19}ClF_{20}P_3Rh$ requires: C, 45.6; H, 1.65; Cl, 3.1; P, 8.0%.

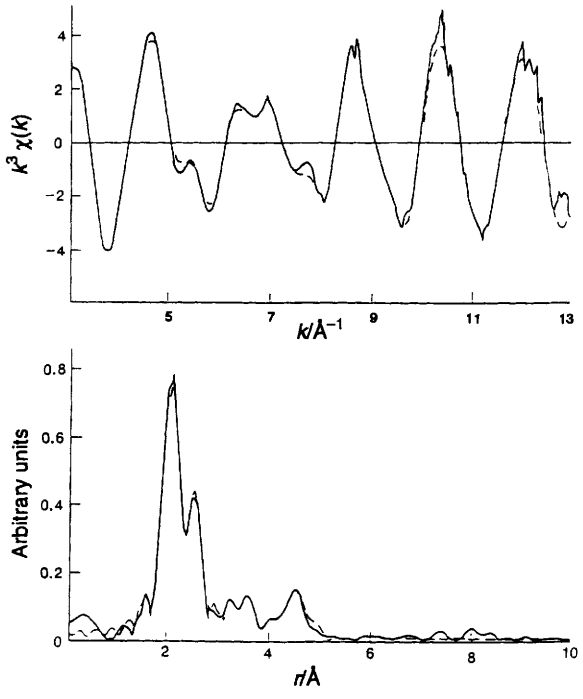

Fig. 1 Background-subtracted EXAFS (——, experimental × k^3; – – –, curved-wave theory × k^3) and the Fourier transform (——, experimental; – – – theoretical) for $[\{Rh(PPh_3)_2(\mu\text{-}Cl)\}_2]$; k is the photoelectron wave vector and r is the radial distance from the absorbing atom

ordination numbers for these shells were modelled by this approach. The AFAC and VPI values were taken from our analysis of $[\{Rh(PPh_3)_2(\mu\text{-}Cl)\}_2]$ and a series of refinements were performed by varying the phosphorus and chlorine occupation numbers simultaneously between 0 and 4 in steps of 0.1. These confirmed that the minima in the fit indices were at 2 ± 0.2. The additional features beyond 3.0 Å were modelled using the same parameter set of non-bonded carbon shells and non-bonded rhodium shell as that used for $[\{Rh(PPh_3)_2(\mu\text{-}Cl)\}_2]$, each shell being added stepwise, iterated in the usual way, and the best fits tested for statistical significance.[13,14] For complexes **2–4** this procedure gave entirely consistent results, particularly for the single Rh···Rh′ non-bonded distance of *ca.* 3.6 Å (Table 3). Again, careful mapping of the co-ordination number of this shell against either of the phosphorus or chlorine shells gave a rhodium occupancy of 1 ± 0.2. However, although the data for complex **1** appeared comparable to that for

Table 2 EXAFS and X-ray crystal data for $[\{Rh(PPh_3)_2(\mu\text{-}Cl)\}_2]$

	Bond lengths[a]		
	X-ray[b]	EXAFS[c]	Debye–Waller factor[a]
d(Rh–P)/Å	2.200(2) 2.213(2)	2.20(0.001)	0.006(0.0001)
d(Rh–Cl)/Å	2.394(2) 2.424(2)	2.37(0.001)	0.011(0.0002)
d(Rh···Rh′)/Å	3.662(2)	3.65(0.004)	0.024(0.002)

[a] Standard deviations in parentheses. [b] Ref. 11. [c] The systematic errors in bond distances arising from the data collection and analysis procedures are *ca.* ±0.02 Å for the first co-ordination shells and *ca.* ±0.04 Å for subsequent shells. Debye–Waller factor given in parentheses. $E0$ 18.94(0.29) eV, fit index $(\Sigma_i[(\chi^T - \chi^E)k_i^3]^2)$ 0.33, R $([\int(\chi^T - \chi^E)k^3dk/\int\chi^Ek^3dk] \times 100\%)$ 15.7, AFAC 0.86, VPI −3.00. Additional non-bonded shells used in fit Rh···C 3.41(1), 0.030(3); 4.10(1), 0.019(2); 4.48(2), 0.015(1).

complexes **2–4**, the additional shells beyond 3.0 Å could not be modelled using the same parameter sets. The best fit to the data (Table 3) gave a significantly longer Rh · · · Rh′ distance of 4.30 Å with a rhodium occupancy of 2 ± 0.2. Fig. 2 shows representative examples of background-subtracted EXAFS and Fourier transforms.

The EXAFS data support the physical and spectroscopic properties and indicate that **1–4** are not monomeric species and have four-co-ordinate, presumably square-planar, rhodium centres comprising two phosphorus and two chlorine atoms.

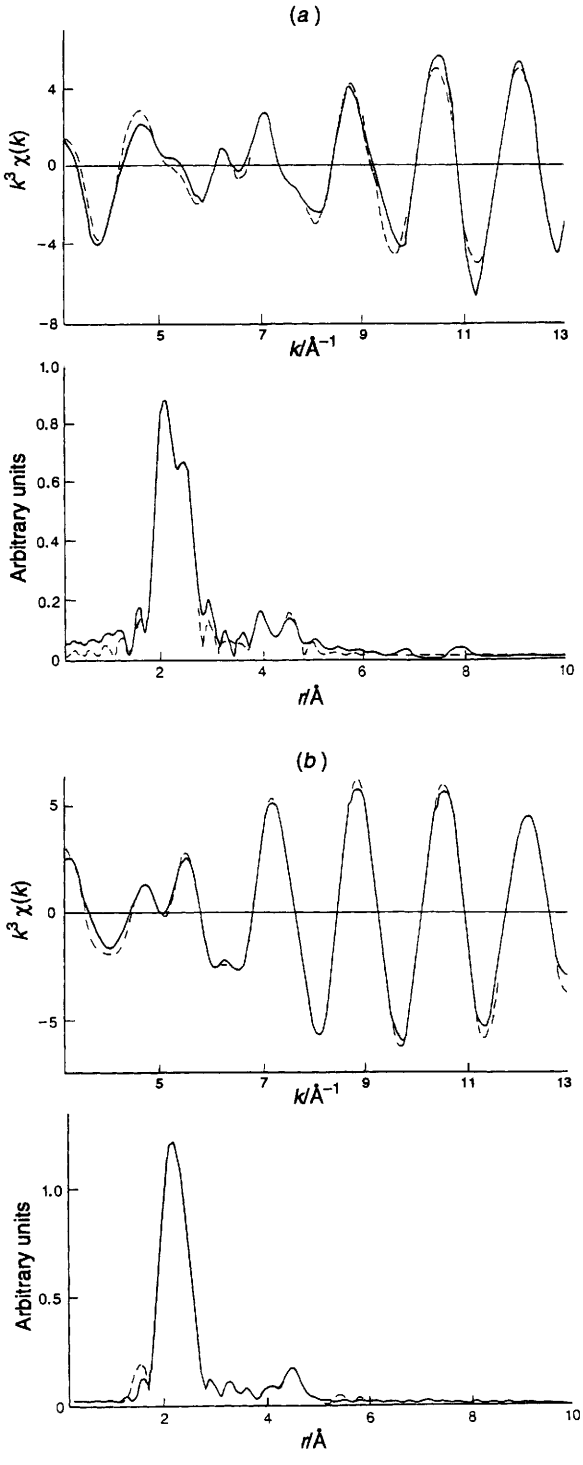

Fig. 2 Background-subtracted EXAFS (——, experimental × k^3; – – –, curved-wave theory × k^3) and the Fourier transforms (——, experimental; – – – theoretical) for (*a*) **1** and (*b*) **4**; *k* is the photoelectron wave vector and *r* is the radial distance from the absorbing atom

The Rh–P distances for **1–4** and for $[\{Rh(PPh_3)_2(\mu\text{-}Cl)\}_2]$ are typical of terminal co-ordinated phosphine ligands. Likewise, the Rh–Cl distances for **1–4** and for $[\{Rh(PPh_3)_2(\mu\text{-}Cl)\}_2]$ are similar and typical of bridging chloride ligands. The only significant differences between the EXAFS data for **1** and **2–4** occur in the non-bonded Rh · · · Rh′ distances. The occupation number and shorter non-bonded Rh · · · Rh′ distance indicate that **2–4** are dinuclear rhodium(I) species, as suggested by mass spectrometry, and the IR and molecular-weight determination studies reported previously.[2] The Rh · · · Rh′ distances of 3.50–3.58 Å are entirely consistent with planar $RhCl_2Rh'$ cores, *cf.* $[\{Rh(\eta^2,\eta^2\text{-}C_8H_{12})(\mu\text{-}Cl)\}_2]$ at 3.498(5) Å[15] and $[\{Rh(PPh_3)_2(\mu\text{-}Cl)\}_2]$ at 3.662(2) Å,[11] and not with the significantly shorter Rh · · · Rh′ distances, < 3.2 Å, typical for dinuclear square-planar rhodium(I) complexes which are folded about the Cl · · · Cl axis.[11]

The polymeric nature of **1** is consistent with its insolubility, the lack of a signal in the mass spectrum and its difference in appearance from the dimeric species. Originally this species was formulated as dimeric, but it was also suggested that it may be a four-co-ordinate rhodium(II) species similar to $[RhCl_2(PPh_3)_2]$[16] and $[RhCl_2\{P(cyclo\text{-}C_6H_{11})_3\}_2]$.[17] Recent magnetic susceptibility measurements confirm the diamagnetism reported previously.[2] The insolubility of the compound is not consistent with monomeric and dimeric tris(pentafluorophenyl)phosphine complexes, which are very soluble in polar organic solvents.[5] Furthermore, the Rh–Cl distances and the previously reported IR spectral data are not consistent with terminal chloride ligands. The available data suggest that the species occurs as a chain in which each Rh · · · Rh′ distance is bridged by just one chloride. The reason for the polymeric nature of the complex may be ascribed to the steric and electronic properties of the tris(pentafluorophenyl)phosphine ligand. The non-basic nature of the ligand prevents stabilisation of the 14-electron, monomeric species, $[RhClL_2]$, which is found for the bulky and σ-donating phosphine $P(cyclo\text{-}C_6H_{11})_3$,[18] but the steric requirements of the ligand prevent the formation of the dimer. The bulk of the ligands prevents a *cis* co-ordination of the chlorides, whereas replacing one C_6F_5 group by C_6H_5 evidently allows such a geometry. The geometry about the rhodium atoms cannot be determined from the EXAFS data, but it is noted that the rhodium, phosphorus and chloride atoms of $[\{Rh(PPh_3)_2(\mu\text{-}Cl)\}_2]$ are coplanar with distorted-square-planar geometry about each rhodium atom [P–Rh–P and Cl–Rh–Cl are 96.34(9) and 81.05(8)° respectively].[11] Presumably, replacement of each C_6H_5 ring of the phosphine by C_6F_5 leads to successively more distortion away

Table 3 EXAFS data for complexes **1–4**[a]

Compound	**1**	**2**	**3**	**4**
d(Rh–P)/Å	2.18 (0.001)	2.19 (0.001)	2.21 (0.001)	2.16 (0.001)
$2\sigma^2$/Å[b]	0.004 (0.0002)	0.006 (0.0002)	0.005 (0.0001)	0.005 (0.0001)
d(Rh–Cl)/Å	2.36 (0.002)	2.38 (0.001)	2.38 (0.001)	2.39 (0.001)
$2\sigma^2$/Å[b]	0.007 (0.0003)	0.009 (0.0002)	0.009 (0.0002)	0.011 (0.0003)
d(Rh · · · Rh′)/Å	4.30 (0.010)	3.58 (0.005)	3.50 (0.009)	3.57 (0.023)
$2\sigma^2$/Å[b]	0.025 (0.002)	0.018 (0.001)	0.026 (0.002)	0.033 (0.004)
Fit index[c]	0.92	0.42	0.32	0.34
R[d]	22.2	15.7	16.5	11.3

[a] Standard deviation in parentheses. Note that the systematic errors in bond distances arising from the data collection and analysis procedures are *ca.* ±0.02 Å for the first co-ordination shells and *ca.* ±0.04 Å for subsequent shells. [b] Debye–Waller factor. [c] Fit index = $\Sigma_i[(\chi^T - \chi^E)k_i^3]^2$. [d] $R = [\int(\chi^T - \chi^E)k^3dk/\int\chi^Ek^3dk] \times 100\%$.

Table 4 Selected bond lengths (Å) and angles (°) with estimated standard deviations (e.s.d.s) in parentheses for $[RhCl(PPh_3)\{(C_6F_5)_2PCH_2CH_2P(C_6F_5)_2\}]\cdot thf$ **9**·thf

Rh–Cl	2.3783(12)	Rh–P(1)	2.2189(12)	C(14)–F(14)	1.335(5)	C(34)–F(34)	1.334(5)
Rh–P(2)	2.1867(12)	Rh–P(3)	2.3709(12)	C(15)–F(15)	1.338(5)	C(35)–F(35)	1.332(5)
P(1)–C(1)	1.830(4)	P(2)–C(2)	1.867(4)	C(16)–F(16)	1.343(5)	C(36)–F(36)	1.345(5)
P(1)–C(11)	1.845(4)	P(1)–C(21)	1.839(4)	C(21)–C(22)	1.374(6)	C(41)–C(42)	1.380(6)
P(2)–C(31)	1.855(4)	P(2)–C(41)	1.851(4)	C(21)–C(26)	1.394(6)	C(41)–C(46)	1.384(6)
P(3)–C(51)	1.838(5)	P(3)–C(61)	1.830(4)	C(22)–C(23)	1.373(6)	C(42)–C(43)	1.379(6)
P(3)–C(71)	1.840(4)	C(1)–C(2)	1.522(6)	C(23)–C(24)	1.358(7)	C(43)–C(44)	1.358(7)
C(11)–C(12)	1.384(6)	C(31)–C(32)	1.394(6)	C(24)–C(25)	1.352(7)	C(44)–C(45)	1.361(7)
C(11)–C(16)	1.369(6)	C(31)–C(36)	1.389(6)	C(25)–C(26)	1.369(6)	C(45)–C(46)	1.382(6)
C(12)–C(13)	1.363(6)	C(32)–C(33)	1.368(6)	C(22)–F(22)	1.348(5)	C(42)–F(42)	1.343(5)
C(13)–C(14)	1.368(7)	C(33)–C(34)	1.359(7)	C(23)–F(23)	1.339(5)	C(43)–F(43)	1.335(5)
C(14)–C(15)	1.367(7)	C(34)–C(35)	1.369(7)	C(24)–F(24)	1.346(5)	C(44)–F(44)	1.346(5)
C(15)–C(16)	1.378(6)	C(35)–C(36)	1.373(6)	C(25)–F(25)	1.351(5)	C(45)–F(45)	1.339(6)
C(12)–F(12)	1.357(5)	C(32)–F(32)	1.328(5)	C(26)–F(26)	1.346(5)	C(46)–F(46)	1.343(5)
C(13)–F(13)	1.341(5)	C(33)–F(33)	1.352(5)				
P(1)–Rh–P(2)	84.44(4)	P(1)–Rh–P(3)	158.32(4)	C(12)–C(11)–C(16)	115.0(4)	C(32)–C(31)–C(36)	115.2(4)
P(2)–Rh–P(3)	102.77(4)	P(1)–Rh–Cl	86.48(4)	C(11)–C(12)–F(12)	119.1(4)	C(31)–C(32)–F(32)	120.9(4)
P(2)–Rh–Cl	165.82(5)	P(3)–Rh–Cl	89.62(4)	C(11)–C(16)–F(16)	121.6(4)	C(31)–C(36)–F(36)	119.5(4)
Rh–P(1)–C(1)	109.7(2)	Rh–P(2)–C(2)	110.68(14)	P(1)–C(21)–C(22)	125.9(4)	P(2)–C(41)–C(42)	117.8(4)
P(1)–C(1)–C(2)	105.5(3)	P(2)–C(2)–C(1)	111.3(3)	P(1)–C(21)–C(26)	119.2(3)	P(2)–C(41)–C(46)	127.5(4)
Rh–P(1)–C(11)	122.4(2)	Rh–P(2)–C(31)	115.0(2)	C(22)–C(21)–C(26)	114.4(4)	C(42)–C(41)–C(46)	114.7(4)
Rh–P(1)–C(21)	113.13(14)	Rh–P(2)–C(41)	125.85(14)	C(21)–C(22)–F(22)	120.2(4)	C(41)–C(42)–F(42)	119.2(4)
C(1)–P(1)–C(11)	98.9(2)	C(2)–P(2)–C(31)	99.9(2)	C(21)–C(26)–F(26)	120.0(4)	C(41)–C(46)–F(46)	121.7(4)
C(1)–P(1)–C(21)	106.5(2)	C(2)–P(2)–C(41)	101.1(2)	Rh–P(3)–C(51)	118.1(2)	Rh–P(3)–C(61)	120.84(14)
C(11)–P(1)–C(21)	104.5(2)	C(31)–P(2)–C(41)	100.6(2)	Rh–P(3)–C(71)	107.6(2)	C(51)–P(3)–C(61)	101.0(2)
P(1)–C(11)–C(12)	123.1(4)	P(2)–C(31)–C(32)	122.4(3)	C(51)–P(3)–C(71)	104.3(2)	C(61)–P(3)–C(71)	103.1(2)
P(1)–C(11)–C(16)	121.5(3)	P(2)–C(31)–C(36)	122.3(4)				

Table 5 Atomic coordinates (× 10^4) for $[RhCl(PPh_3)\{(C_6F_5)_2PCH_2CH_2P(C_6F_5)_2\}]\cdot thf$ **9**·thf

Atom	*x*	*y*	*z*	Atom	*x*	*y*	*z*
Rh	4186(1)	1721(1)	1832(1)	C(61)	2124(4)	2096(3)	445(2)
Cl	4926(1)	437(1)	1899(1)	C(62)	1095(4)	2096(3)	581(2)
P(1)	5632(1)	2066(1)	2522(1)	C(63)	327(4)	2615(4)	284(3)
P(2)	3587(1)	2880(1)	2020(1)	C(64)	559(5)	3127(3)	−150(3)
P(3)	3122(1)	1404(1)	852(1)	C(65)	1577(5)	3144(3)	−278(3)
C(1)	5757(3)	3135(2)	2543(2)	C(66)	2355(4)	2627(3)	23(2)
C(2)	4639(3)	3443(2)	2558(2)	C(71)	4034(4)	1271(3)	306(2)
C(11)	5759(4)	1883(3)	3360(2)	C(72)	3697(5)	1047(4)	−302(3)
C(12)	6658(4)	2090(3)	3796(2)	C(73)	4420(6)	913(4)	−683(3)
C(13)	6719(5)	2037(3)	4420(2)	C(74)	5470(6)	1006(3)	−475(3)
C(14)	5849(5)	1764(3)	4635(2)	C(75)	5805(5)	1252(5)	107(3)
C(15)	4939(4)	1551(3)	4226(2)	C(76)	5097(4)	1372(4)	502(3)
C(16)	4915(4)	1607(3)	3599(2)	F(12)	7538(2)	2361(2)	3601(1)
C(21)	6887(3)	1685(3)	2339(2)	F(13)	7624(3)	2234(2)	4816(1)
C(22)	7480(4)	1070(3)	2631(2)	F(14)	5903(3)	1695(2)	5245(1)
C(23)	8375(4)	778(3)	2449(2)	F(15)	4085(3)	1286(2)	4436(1)
C(24)	8671(4)	1069(3)	1933(3)	F(16)	3990(2)	1384(2)	3232(1)
C(25)	8102(4)	1660(3)	1616(2)	F(22)	7206(2)	733(2)	3132(1)
C(26)	7229(4)	1961(3)	1814(2)	F(23)	8931(2)	195(2)	2770(2)
C(31)	2507(3)	2876(3)	2477(2)	F(24)	9542(3)	789(2)	1742(2)
C(32)	1893(4)	2213(3)	2532(2)	F(25)	8393(3)	1952(2)	1103(1)
C(33)	1138(4)	2212(3)	2897(2)	F(26)	6680(2)	2535(2)	1470(1)
C(34)	935(4)	2864(4)	3209(2)	F(32)	2019(2)	1558(2)	2227(1)
C(35)	1519(4)	3530(3)	3173(2)	F(33)	577(3)	1549(2)	2945(2)
C(36)	2282(4)	3526(3)	2810(2)	F(34)	167(3)	2857(2)	3544(2)
C(41)	3074(4)	3635(2)	1432(2)	F(35)	1335(3)	4177(2)	3475(1)
C(42)	3799(4)	3986(3)	1127(2)	F(36)	2797(2)	4205(2)	2763(1)
C(43)	3534(5)	4578(3)	697(2)	F(42)	4827(2)	3748(2)	1249(1)
C(44)	2503(6)	4837(3)	563(2)	F(43)	4282(3)	4897(2)	425(1)
C(45)	1743(5)	4507(3)	840(2)	F(44)	2226(3)	5424(2)	155(1)
C(46)	2032(4)	3909(3)	1264(2)	F(45)	728(3)	4764(2)	704(1)
C(51)	2332(4)	495(3)	784(2)	F(46)	1232(2)	3612(2)	1511(1)
C(52)	1745(5)	245(3)	229(3)	H(76A)	5347(4)	1808(4)	927(3)
C(53)	1216(5)	−469(4)	182(3)	C(3)	2465(9)	9675(5)	3014(5)
C(54)	1213(5)	−910(3)	695(3)	C(4)	2332(9)	9766(6)	3629(4)
C(55)	1753(5)	−657(3)	1250(3)	C(5)	1451(7)	9242(7)	3666(4)
C(56)	2320(4)	46(3)	1296(2)	C(6)	1156(6)	8855(6)	3079(4)
				O(1)	2020(6)	8963(4)	2787(3)

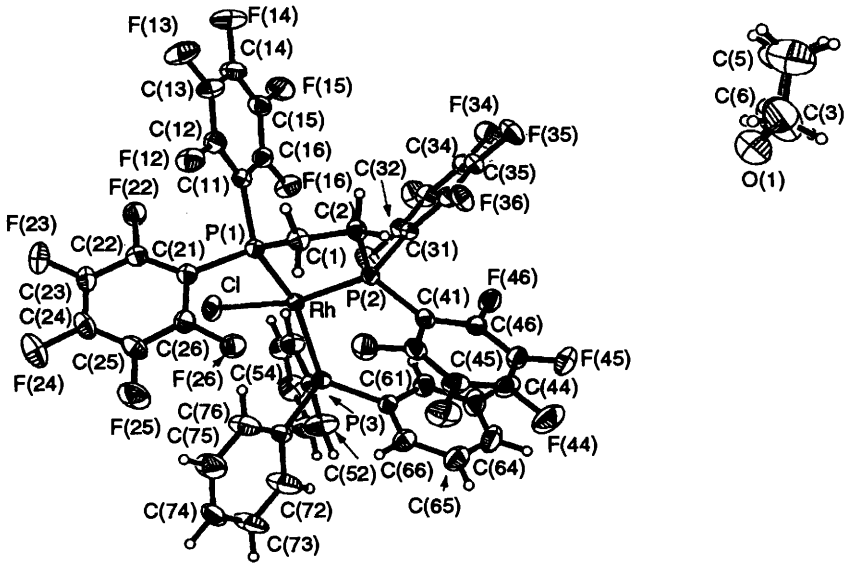

Fig. 3 Molecular structure of [RhCl(PPh$_3$)(dfppe)]·thf **9**·thf. Displacement ellipsoids are shown at the 30% probability level

from *cis* square-planar geometry. The geometries of bis{tris-(pentafluorophenyl)phosphine} complexes of platinum[19,20] and iridium[21] have been determined to be *trans* square-planar or distorted *trans* square-planar. Presumably complex **1** possesses a similar geometry about the rhodium atom.

The complexes [Rh{PPh$_x$(C$_6$F$_5$)$_{3-x}$}$_2$Cl(CO)] (x = 0 **5**, 1 **6** or 2 **7**) were prepared by treatment of [{Rh(CO)$_2$(μ-Cl)}$_2$] with the respective phosphine. Complex **5** was also prepared by bubbling carbon monoxide through a slurry of complex **1**. These three are all yellow solids, readily soluble in polar organic solvents. They were characterized by comparison of their ν(C≡O) resonances with those reported,[2] and also by mass spectrometry and ^{1}H, ^{19}F and ^{31}P-{^{1}H} NMR spectroscopies (Table 1). The data indicate that, as expected, the complexes are mononuclear and confirms the *trans*-square-planar or distorted-square-planar geometries, as found for [IrCl(CO)(PPh$_3$)$_2$][22] and [IrBr(CO){P(C$_6$F$_5$)$_3$}$_2$].[21] The values of ν(C≡O) increase in the order **7** < **6** < **5** demonstrating the electron-withdrawing nature of the C$_6$F$_5$ moiety. For comparison, *trans*-[RhCl(CO)(PPh$_3$)$_3$] exhibits ν(C≡O) at 1965 cm^{-1}.[23] All three complexes exhibit doublet resonances in their ^{31}P-{^{1}H} NMR spectra shifted to higher frequency by *ca.* 50 ppm from those of the free ligands. The values of ^1J(RhP) for compounds **6** and **7** are *ca.* 135 Hz, whilst that of the compound **5** is *ca.* 20 Hz larger. The ^{31}P-{^{1}H} NMR spectra confirm the *trans* disposition of the phosphine ligands of **5**–**7**.

The reaction between [{Rh(CO)$_2$(μ-Cl)}$_2$] and dfppe in dichloromethane at room temperature yields a mixture of complex **4** and a carbonyl-containing species, **8**. The ^{31}P-{^{1}H} NMR and IR spectral data are consistent with the formulation *cis*-[Rh{(C$_6$F$_5$)$_2$PCH$_2$CH$_2$P(C$_6$F$_5$)$_2$}Cl(CO)]. Solutions of complex **8** readily lose carbon monoxide on warming to give **4**.

Treatment of complex **4** with PPh$_3$ in dichloromethane gave the four-co-ordinate rhodium(I) complex [RhCl(PPh$_3$)(dfppe)] **9** in *ca.* 30% yield (Scheme 1). Complex **9** was characterized by elemental analysis, mass spectrometry, IR and NMR spectroscopies. The ^{19}F NMR spectrum exhibits two sets of *ortho*- and *para*-fluorine resonances, consistent with a square-planar geometry. The ^{31}P-{^{1}H} NMR spectrum displays a complicated, second-order ABCX spectrum centred at δ 33.0. This is consistent with a square-planar geometry with three non-equivalent phosphorus atoms coupled to each other. The spectrum is further complicated by phosphorus–fluorine coupling. Attempts to simulate this spectrum have been unsuccessful. Complex **9** can also be formed by the reaction between [Rh(C$_6$H$_5$)Cl$_2$(PPh$_3$)$_2$][24] and dfppe, which proceeds *via* reductive elimination of chlorobenzene, as evidenced by ^{1}H NMR spectroscopy.

Complex **9** was further characterized by X-ray crystallography. The structure of [RhCl(PPh$_3$)(dfppe)]·thf is shown in Fig. 3. Selected bond lengths and angles are given in Table 4 and atomic coordinates in Table 5. Complex **9** exhibits tetrahedrally distorted-square-planar geometry about the rhodium atom, similar to that found in [RhCl(PPh$_3$)$_3$],[25,26] such that the dihedral angle between the plane containing the two dfppe phosphorus atoms and the rhodium atom and the plane containing the chloride, the triphenylphosphine phosphorus and rhodium atoms is 23.24°. The distance between the rhodium atom and one of the *ortho*-hydrogen atoms of one phenyl ring is short [Rh · · · H(76) 2.699 Å]. This is indicative of a 'non-primary valence interaction'[25] or weak agostic interaction.[27] The structure is therefore similar to that of the red form of [RhCl(PPh$_3$)$_3$], where there is a short Rh · · · H distance of 2.77 Å between the rhodium atom and one of the *ortho*-hydrogen atoms of one of the phenyl rings of a phosphine *cis* to the chloride. The next closest hydrogen is at 3.143 Å, and the two closest fluorines are at 3.064 [F(32)] and 3.189 Å [F(16)]. The Rh–P(3) (PPh$_3$) bond is *ca.* 0.18 Å longer than the Rh–P(dfppe) bonds, and Rh–P(1) (P *trans*-PPh$_3$) is longer than Rh–P(2) (P *trans*-Cl) by 0.03 Å. The Rh–P(3) bond is slightly longer than those of 2.334(3) and 2.324(4) Å for Rh–P(*cis*-Cl) in the red form of [RhCl(PPh$_3$)$_3$]. The Rh–Cl bond length of 2.3783(12) Å is intermediate between those of the orange and red forms of [RhCl(PPh$_3$)$_3$]. These values are consistent with the π-acidity, and thus the *trans* effect of phosphorus being greater than that of chloride, and also that of dfppe being greater than that of PPh$_3$, but may also be a consequence of the steric pressure exerted by the bulky dfppe ligand.[28]

The P–Rh–P angle for the dfppe ligand is 84.44(4)°, which is less than those of [Mo(η^5-C$_5$H$_5$)(dfppe)(CO)Cl] [86.8(1)°],[29] and [Pt(dfppe)$_2$] [89.4(1) and 89.6(1)°].[30] The Rh(PCH$_2$)$_2$ five-membered ring is distorted from C_2 symmetry, P(1)–C(1) being 0.037 Å shorter than P(2)–C(2). The two Rh–P–C angles are similar at *ca.* 110°, but the two P–C–C angles differ by *ca.* 6°, the smaller P–C–C angle being associated with the shorter P–C bond. The C–C bond length is similar to that of dfppe. The geometries about each of the two dfppe phosphorus atoms are distorted tetrahedral. The three Rh–P(1)–C angles range from 109.7(2) to 122.4(2)°, and those for Rh–P(2)–C range from 110.68(14) to 125.85(14)°. The P(1)–C(C$_6$F$_5$) distances are slightly shorter than that of P(2)–C(C$_6$F$_5$). There is one P–C–C(C$_6$F$_5$) angle significantly less than 120°, with the other seven ranging from 119 to 128°.

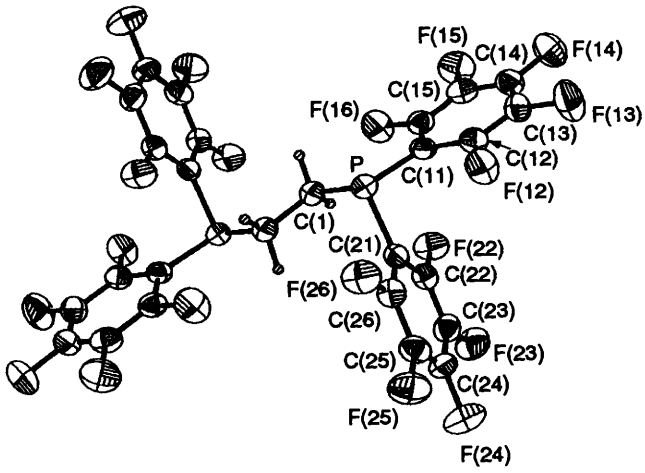

Fig. 4 Molecular structure of $(C_6F_5)_2PCH_2CH_2P(C_6F_5)_2$. Displacement ellipsoids are shown at the 30% probability level

Table 6 Bond lengths (Å) and angles (°) with e.s.d.s in parentheses for $(C_6F_5)_2PCH_2CH_2P(C_6F_5)_2$

P–C(1)	1.840(4)	C(1)–C(1)′	1.520(8)
P–C(11)	1.846(4)	P–C(21)	1.846(4)
C(11)–C(12)	1.383(5)	C(21)–C(22)	1.394(5)
C(11)–C(16)	1.389(5)	C(21)–C(26)	1.377(5)
C(12)–C(13)	1.375(5)	C(22)–C(23)	1.369(5)
C(13)–C(14)	1.369(6)	C(23)–C(24)	1.377(6)
C(14)–C(15)	1.359(6)	C(24)–C(25)	1.360(6)
C(15)–C(16)	1.375(6)	C(25)–C(26)	1.385(6)
C(12)–F(12)	1.348(4)	C(22)–F(22)	1.336(4)
C(13)–F(13)	1.333(4)	C(23)–F(23)	1.346(5)
C(14)–F(14)	1.339(4)	C(24)–F(24)	1.332(5)
C(15)–F(15)	1.352(4)	C(25)–F(25)	1.338(4)
C(16)–F(16)	1.331(4)	C(26)–F(26)	1.341(4)
C(1)′–C(1)–P	109.1(4)	C(1)–P–C(11)	105.0(2)
C(1)–P–C(21)	100.1(2)	C(11)–P–C(21)	100.2(2)
P–C(11)–C(12)	116.7(3)	P–C(21)–C(22)	125.2(3)
P–C(11)–C(16)	127.9(3)	P–C(21)–C(26)	119.2(3)
C(12)–C(11)–C(16)	114.9(4)	C(22)–C(21)–C(26)	115.6(4)
C(11)–C(12)–C(13)	123.8(4)	C(21)–C(22)–C(23)	122.2(4)
C(12)–C(13)–C(14)	119.1(4)	C(22)–C(23)–C(24)	120.1(4)
C(13)–C(14)–C(15)	119.2(4)	C(23)–C(24)–C(25)	119.7(4)
C(14)–C(15)–C(16)	120.9(4)	C(24)–C(25)–C(26)	119.2(4)
C(15)–C(16)–C(11)	122.1(4)	C(25)–C(26)–C(21)	123.2(4)
C(11)–C(12)–F(12)	118.8(3)	C(21)–C(22)–F(22)	120.4(3)
C(13)–C(12)–F(12)	117.4(4)	C(23)–C(22)–F(22)	117.4(4)
C(12)–C(13)–F(13)	120.9(4)	C(22)–C(23)–F(23)	120.3(4)
C(14)–C(13)–F(13)	120.0(4)	C(24)–C(23)–F(23)	119.6(4)
C(13)–C(14)–F(14)	120.0(4)	C(23)–C(24)–F(24)	120.0(4)
C(15)–C(14)–F(14)	120.8(4)	C(25)–C(24)–F(24)	120.3(4)
C(14)–C(15)–F(15)	119.4(4)	C(24)–C(25)–F(25)	120.4(4)
C(16)–C(15)–F(15)	119.6(4)	C(26)–C(25)–F(25)	120.4(4)
C(15)–C(16)–F(16)	116.8(4)	C(25)–C(26)–F(26)	116.7(4)
C(11)–C(16)–F(16)	121.2(4)	C(21)–C(26)–F(26)	120.2(3)

The geometry about the PPh_3 phosphorus atom is similar to that of the PPh_3 ligand which is *cis* to chloride and shows a close approach of an *ortho*-hydrogen atom to rhodium in the red form of $[RhCl(PPh_3)_3]$.

The structure of dfppe is shown in Fig. 4. It adopts a similar structure to those of both forms of dppe,[31] with the centre of the C(1)–C(1)′ bond on a crystallographic centre of symmetry. Bond lengths and angles are given in Table 6, atomic coordinates in Table 7. The molecule adopts a *trans* configuration about the C–C bond. The geometry about the phosphorus atom is distorted trigonal pyramidal, the three C–P–C angles being significantly less than the tetrahedral angle (109.5°); two of these angles are similar, but the third is *ca.* 5° larger. Thus dfppe differs from dppe in which all the C–P–C angles are close to 100°. The P–C(1)–C(1)′ angle is slightly smaller than that of dppe. The C(1)–C(1)′ bond length is similar to those of 1.516(4) and 1.530(5) in dppe. The P–C(1) bond length is similar to that for both forms of dppe, while the other P–C bond lengths are between 0.009 and 0.028 Å longer. Thus dfppe adopts a similar geometry about the phosphorus atoms to dppe, but with longer P–C(sp^2) bonds.

Table 7 Atomic coordinates (× 10^4) for $(C_6F_5)_2PCH_2CH_2P(C_6F_5)_2$

Atom	*x*	*y*	*z*
P	2 898(2)	8 921(1)	4 023(1)
C(1)	5 321(8)	9 318(4)	4 834(4)
C(11)	3 994(7)	7 367(4)	3 520(3)
C(12)	2 547(7)	6 911(4)	2 799(3)
C(13)	2 999(7)	5 690(4)	2 459(4)
C(14)	4 972(8)	4 853(4)	2 860(4)
C(15)	6 455(7)	5 262(4)	3 565(4)
C(16)	5 981(7)	6 488(4)	3 894(3)
C(21)	3 020(7)	10 271(4)	2 598(3)
C(22)	4 842(7)	10 369(4)	1 785(3)
C(23)	4 823(7)	11 402(4)	743(4)
C(24)	2 956(8)	12 382(4)	463(4)
C(25)	1 139(7)	12 327(4)	1 230(4)
C(26)	1 197(7)	11 278(4)	2 282(3)
F(12)	586(4)	7 705(3)	2 388(2)
F(13)	1 544(5)	5 316(3)	1 751(3)
F(14)	5 414(5)	3 646(3)	2 559(3)
F(15)	8 407(4)	4 439(3)	3 962(3)
F(16)	7 510(4)	6 791(3)	4 605(2)
F(22)	6 686(4)	9 436(3)	2 001(2)
F(23)	6 604(5)	11 448(3)	−26(2)
F(24)	2 952(5)	13 394(3)	−546(2)
F(25)	−684(4)	13 276(3)	972(2)
F(26)	−633(4)	11 280(3)	3 008(2)

Experimental

The ^1H, ^{19}F and ^{31}P NMR spectra were recorded in $CDCl_3$ on a Bruker AM 300 spectrometer at 300.14, 282.36 and 121.50 MHz respectively; ^1H NMR spectra were referenced internally using the residual protio solvent resonance relative to tetramethylsilane (δ 0); ^{19}F NMR spectra referenced externally to $CFCl_3$ (δ 0) and ^{31}P NMR spectra referenced externally to 85% H_3PO_4 (δ 0).

Infrared spectra were recorded as Nujol mulls between KBr plates on a Digilab FTS40 Fourier-transform spectrometer. Data are expressed in wavenumbers (cm^{-1}) with relative intensities (s = strong, m = medium, w = weak). Elemental analyses were performed by Butterworth Laboratories Ltd and FAB mass spectra were recorded on a Kratos Concept 1H mass spectrometer.

The complexes $[\{Rh[P(C_6F_5)_3]_2Cl\}_n]$, $[\{Rh[PPh(C_6F_5)_2]_2Cl\}_2]$, $[\{Rh[PPh_2(C_6F_5)]_2Cl\}_2]$, $[Rh\{P(C_6F_5)_3\}_2Cl(CO)]$, $[Rh\{PPh(C_6F_5)_2\}_2Cl(CO)]$ and $[Rh\{PPh_2(C_6F_5)\}_2Cl(CO)]$ were prepared as previously described;[2] $[\{Rh(\eta\text{-}C_2H_4)_2Cl\}_2]$ and $[\{Rh(CO)_2Cl\}_2]$ (Aldrich) and $PPh_2(C_6F_5)$, $PPh(C_6F_5)_2$, $P(C_6F_5)_3$ and $(C_6F_5)_2PCH_2CH_2P(C_6F_5)_2$ (Fluorochem) were used as supplied.

Preparations.—Bis{bis(dipentafluorophenylphosphino)ethane}di-μ-chlorodirhodium **4**. A mixture of $[\{Rh(\eta\text{-}C_2H_4)_2Cl\}_2]$ (0.086 g, 0.22 mmol) and dfppe (0.352 g, 0.46 mmol) in methanol (30 cm^3) was refluxed under nitrogen for 2 h. The mixture was allowed to cool and the orange solid was filtered, washed with methanol (10 cm^3) and light petroleum (b.p. 40–60 °C, 5 cm^3), and dried *in vacuo*. Yield: 0.244 g, 62%. IR: 1644m, 1522s, 1480s, 1418w, 1390m, 1280m, 1146w, 1093s, 1023w, 972s, 891w, 842w, 760w, 726w, 655w, 635w, 586w, 530m, 470w cm^{-1}.

Table 8 X-Ray crystal data collection, solution and refinement details for $[RhCl(PPh_3)\{(C_6F_5)_2PCH_2CH_2P(C_6F_5)_2\}]\cdot thf$ **9**·thf and $(C_6F_5)_2PCH_2CH_2P(C_6F_5)_2$[a]

Compound	**9**·thf	$(C_6F_5)_2PCH_2CH_2P(C_6F_5)_2$
Formula	$C_{48}H_{27}ClF_{20}OP_3Rh$	$C_{26}H_4F_{20}P_2$
M	1230.97	758.24
Crystal size/mm	0.29 × 0.28 × 0.22	0.25 × 0.16 × 0.13
Crystal system	Monoclinic	Triclinic
Space group	$P2_1/c$	$P\bar{1}$
a/Å	12.707(2)	5.833(1)
b/Å	17.066(2)	10.011(2)
c/Å	22.003(3)	11.514(4)
α/°	90	75.25(2)
β/°	101.41(1)	88.69(2)
γ/°	90	84.28(2)
U/Å^3	4677.2(11)	647.0(3)
Z	4	1
D_c/g cm^{-3}	1.748	1.946
μ/mm^{-1}	0.644	0.333
$F(000)$	2440	370
Scan width	±0.5° (ω)[b]	±0.6° (ω)[b]
Total data	8982	2246
Unique data, R_{int}	7269, 0.0237	2019, 0.0316
Observed data [$I > 2\sigma(I)$]	5193	1339
Least squares variables	667	217
R_1, wR_2 [$I > 2\sigma(I)$][c]	0.0429, 0.0715	0.0482, 0.0987
R_1, wR_2 (all data)	0.0747, 0.0824	0.0884, 0.1171
Goodness of fit, F^2[d]	1.027	1.034
Difference map features/e Å^{-3}	+0.302, −0.333	+0.209, −0.288

[a] Details in common: Siemens P4 diffractometer, λ(Mo-Kα) = 0.7107 Å, 2θ range 5–48°, ω scan type. [b] Around the Kα1–Kα2 angles. [c] $R_1 = \Sigma||F_o| - |F_c||/\Sigma|F_o|$; $wR_2 = \{\Sigma[w(F_o^2 - F_c^2)^2]/\Sigma[w(F_o^2)^2]\}^{\frac{1}{2}}$. [d] Goodness of fit, $S = \{\Sigma[w(F_o^2 - F_c^2)^2/(n-p)]\}^{\frac{1}{2}}$, where n = number of reflections and p is the total number of parameters refined.

cis-{*Bis(dipentafluorophenylphosphino)ethane*}*carbonylchlororhodium* **8**. The complex $[\{Rh(CO)_2Cl\}_2]$ (0.021 g, 0.054 mmol) and the phosphine dfppe (0.090 g, 0.108 mmol) were dissolved in dichloromethane (30 cm^3) under nitrogen to give an immediate yellow solution with evolution of a colourless gas. After stirring for 15 min, the solvent was removed by rotary evaporation to yield a yellow-orange solid, which was dried *in vacuo* to give 0.081 g of crude product, which NMR and IR spectroscopies showed was a mixture of *cis*-$[Rh\{(C_6F_5)_2PCH_2CH_2P(C_6F_5)_2\}Cl(CO)]$ **4** and $[\{Rh(CO)_2Cl\}_2]$.

{*Bis(dipentafluorophenylphosphino)ethane*}*chlorotriphenylphosphinerhodium* **9**. Triphenylphosphine (0.028 g, 0.11 mmol) was added to a solution of complex **4** (0.079 g, 0.044 mmol) in dichloromethane (20 cm^3) at room temperature. After 24 h light petroleum (b.p. 40–60 °C; 20 cm^3) was added to precipitate a white solid. The solution was filtered and the solvent removed by rotary evaporation to yield a yellow solid. The solid was extracted with light petroleum (50 cm^3) and the resulting yellow solution was filtered. On evaporation of the solvent the product was obtained as a yellow solid. Yield: 0.028 g, 27%. IR: 1644m, 1521s, 1478s, 1438w, 1384m, 1290m, 1139w, 1093s, 1072w, 1026w, 979s, 893w, 842w, 833w, 747w, 725w, 696m, 632w, 529m, 506m cm^{-1}.

EXAFS Determinations of **1**–**4**.—The purity of samples prepared for EXAFS was checked by elemental analysis (complexes **1** and **4**), and by NMR spectroscopy (**2** and **3**). Only uncomplexed phosphine, which would not significantly affect the EXAFS data, was observed in the NMR spectra of **2** and **3**.

Rhodium K-edge EXAFS data were collected at the Daresbury Synchrotron Radiation Source at 2 GeV (*ca.* 3.2 × 10^{-10} J) with an average current of 190 mA in transmission mode on station 9:2 using a double-crystal Si(220) monochromator offset to 50% of the rocking curve for harmonic rejection. The samples were diluted with dry boron nitride and mounted between Sellotape strips in 1 mm aluminium spacers. The EXAFS data treatment utilised the programs EX[32] and EXCURV90.[33] Several data sets were collected for each compound in k space, and averaged to improve the signal-to-noise ratio. The pre-edge background was removed by fitting the spectum to a quadratic polynomial, and subtracting this from the whole spectrum. The atomic contribution to the oscillatory part of the absorption spectrum was approximated using polynomials, and the optimum function judged by minimising the intensity of chemically insignificant shells at low r in the Fourier transform. Curve fitting used single-scattering curved-wave theory with phase shifts and back-scattering factors calculated using the normal *ab initio* methods.[34]

X-Ray Crystal Structure Determinations of **9** *and* $(C_6F_5)_2PCH_2CH_2P(C_6F_5)_2$.—Crystals of **9** and dfppe, suitable for diffraction, were grown from thf–diethyl ether and dichloromethane respectively. The crystal data and experimental parameters for both compounds are given in Table 8. Unit-cell parameters for **9** were determined from the optimised setting angles of 34 reflections in the range 10 < 2θ < 24° and for dfppe from 24 reflections in the range 8 < 2θ < 25°. A semi-empirical absorption correction was applied to the data for **9** (based on psi scans), and the data for both structures were corrected for Lorentz and polarisation effects. Both structures were solved using SHELXTL-pc[35] and refined using the program package SHELXL-93,[36] and crystal stability was monitored by the observation of the intensities of three standard reflections and for neither structure was there any significant loss of intensity.

The structure of the complex **9** was solved by Patterson and Fourier methods. All non-hydrogen atoms were refined with anisotropic thermal parameters. The agostic hydrogen atom, H(76), was located on a difference Fourier map and included in the refinement cycles constrained to ride on C(76). All other hydrogen atoms were included in calculated positions (C–H 0.96 Å) with a fixed isotropic thermal parameter (U_{iso} = 0.08 Å^2).

The structure of dfppe was solved by direct methods. Only one molecule of dfppe is found in the unit cell, with the centre of the C–C bond linking the two phosphorus atoms on a centre

of symmetry. All non-hydrogen atoms were refined with anisotropic thermal parameters. The hydrogen atoms bonded to C(1) were included in calculated positions (C–H 0.96 Å) with fixed isotropic thermal parameters (U_{iso} = 0.05 Å^2).

The final atomic positional parameters for **9** and dfppe are given in Tables 5 and 7 respectively. Additional material, available from the Cambridge Crystallographic Data Centre, comprises hydrogen atom coordinates, thermal parameters and remaining bond lengths and angles.

Acknowledgements

We thank the Director of Daresbury laboratory for provision of facilities, Dr. A. K. Brisdon for assistance with the EXAFS data collection and analysis, Dr. G. Eaton for recording mass spectra, S. Barlow for the magnetic measurements, the University of Leicester for provision to purchase a four-circle X-ray diffractometer, Dr. R. D. W. Kemmitt for helpful discussion and BNFL Fluorochemicals Ltd. (G. C. S.) and the EPSRC (K. S. C., E. G. H. and L. A. P.) for support.

References

1 R. D. W. Kemmitt, D. I. Nichols and R. D. Peacock, *J. Chem. Soc., Chem. Commun.*, 1967, 599.
2 R. D. W. Kemmitt, D. I. Nichols and R. D. Peacock, *J. Chem. Soc. A*, 1968, 1898.
3 R. D. W. Kemmitt, D. I. Nichols and R. D. Peacock, *J. Chem. Soc. A*, 1968, 2149.
4 I. Ojima and H. B. Kwon, *J. Am. Chem. Soc.*, 1988, **110**, 5617.
5 A. K. Brisdon, J. H. Holloway, E. G. Hope, D. R. Russell, G. C. Saunders, R. M. J. Stead and M. J. Atherton, unpublished work.
6 J. H. Holloway, E. G. Hope, K. Jones, G. C. Saunders, J. Fawcett, N. Reeves, D. R. Russell and M. J. Atherton, *Polyhedron*, 1993, **12**, 2681.
7 K. S. Coleman, J. H. Holloway, E. G. Hope, G. C. Saunders, D. R. Russell and M. J. Atherton, *Polyhedron*, 1995, **14**, 2701.
8 D. I. Nichols, *J. Chem. Soc. A*, 1969, 1471.
9 A. J. Naaktgeboren, R. J. M. Nolte and W. Drenth, *J. Am. Chem. Soc.*, 1980, **102**, 3350.
10 See for example: S. K. Harbron, S. J. Higgins, W. Levason, M. C. Feiters and A. T. Steel, *Inorg. Chem.*, 1986, **25**, 1789; L. R. Hanton, J. Evans, W. Levason and R. J. Perry, *J. Chem. Soc., Dalton Trans.*, 1991, 2039.
11 M. D. Curtis, W. M. Butler and J. Greene, *Inorg. Chem.*, 1978, **17**, 2928.
12 I. R. Beattie, P. J. Jones and N. A. Young, *J. Am. Chem. Soc.*, 1992, **114**, 6146.
13 R. W. Joyner, K. J. Martin and P. Meehan, *J. Phys. C*, 1987, **20**, 4005.
14 N. Binsted, S. L. Cook, J. Evans, G. N. Greaves and R. J. Price, *J. Am. Chem. Soc.*, 1987, **109**, 3667.
15 J. A. Ibers and R. G. Snyder, *Acta Crystallogr.*, 1962, **15**, 923.
16 C. A. Ogle, T. C. Masterman and J. L. Hubbard, *J. Chem. Soc., Chem. Commun.*, 1990, 1733.
17 F. G. Moers, J. A. M. de Jong and P. M. H. Beaumont, *J. Inorg. Nucl. Chem.*, 1973, **35**, 1915.
18 H. L. M. Van Gaal and F. L. A. Van den Bekerom, *J. Organomet. Chem.*, 1977, **134**, 237.
19 W. N. Hunter, K. W. Muir and D. W. A. Sharp, *Acta Crystallogr., Sect. C*, 1986, **42**, 1743.
20 W. P. Schaefer, D. K. Lyon, J. A. Labinger and J. E. Bercaw, *Acta Crystallogr., Sect. C*, 1992, **48**, 1582.
21 J. H. Holloway, E. G. Hope, D. R. Russell, G. C. Saunders and M. J. Atherton, *Polyhedron*, in the press.
22 M. R. Churchill, J. C. Fettinger, L. A. Buttrey, M. D. Barkan and J. S. Thompson, *J. Organomet. Chem.*, 1988, **340**, 257.
23 J. Blum, E. Oppenheimer and E. D. Bergmann, *J. Am. Chem. Soc.*, 1967, **89**, 2338.
24 J. Fawcett, J. H. Holloway and G. C. Saunders, *Inorg. Chim. Acta*, 1992, **202**, 111.
25 M. J. Bennet, P. B. Donaldson, P. B. Hitchcock and R. Mason, *Inorg. Chim. Acta*, 1975, **12**, L9.
26 M. J. Bennett and P. B. Donaldson, *Inorg. Chem.*, 1977, **16**, 655.
27 M. Brookhart, M. L. H. Green and L.-L. Wong, *Prog. Inorg. Chem.*, 1988, **36**, 1.
28 W. D. Horrocks, jun. and R. C. Taylor, *Inorg. Chem.*, 1963, **2**, 723; R. Mason and A. D. C. Towl, *J. Chem. Soc. A*, 1970, 1601.
29 M. F. Ernst and D. M. Roddick, *Inorg. Chem.*, 1990, **29**, 3627.
30 R. K. Merwin, R. C. Schnabel, J. D. Koola and D. M. Roddick, *Organometallics*, 1992, **11**, 2972.
31 C. Pelizzi and G. Pelizzi, *Acta Crystallogr., Sect. B*, 1979, **35**, 1785.
32 A. K. Brisdon, EX-A Program For EXAFS Data Reduction, University of Leicester, 1992.
33 N. Binsted, S. J. Gurman and J. W. Campbell, EXCURV90, SERC Daresbury Laboratory Program, 1990.
34 S. J. Gurman, N. Binsted and I. Ross, EXCURVE, *J. Phys. C*, 1984, **17**, 143; 1986, **19**, 1845.
35 G. M. Sheldrick, SHELXTL-pc Release 4.2, Siemens Analytical X-ray Instruments, Madison, WI, 1991.
36 G. M. Sheldrick, SHELXL-93, Program for Crystal Structure Refinement, University of Göttingen, 1993.

Received 27*th July* 1995; *Paper* 5/04572J